

Effect of pinning and driving force on the metastability effects in weakly pinned superconductors and the determination of spinodal line pertaining to order–disorder transition

A D THAKUR^{1,*}, S S BANERJEE^{2,†}, M J HIGGINS³, S RAMAKRISHNAN¹
and A K GROVER¹

¹DCMP&MS, Tata Institute of Fundamental Research, Mumbai 400 005, India

²Department of Physics, Indian Institute of Technology, Kanpur 208 076, India

³NEC Research Institute, Princeton, New Jersey 08540, USA

E-mail: *ajay@tifr.res.in; [†]satyajit@iitk.ac.in

Abstract. We explore the effect of varying drive on metastability features exhibited by the vortex matter in single crystals of 2H-NbSe₂ and CeRu₂ with varying degree of random pinning. The metastable nature of vortex matter is reflected in the path dependence of the critical current density, which in turn is probed in a contact-less way via AC-susceptibility measurements. The sinusoidal AC magnetic field applied during AC susceptibility measurements appears to generate a driving force on the vortex matter. In a nascent pinned single crystal of 2H-NbSe₂, where the peak effect (PE) pertaining to the order–disorder phenomenon is a sharp first-order-like transition, the supercooling feature below the peak temperature is easily wiped out by the reorganization caused by the AC driving force. In this paper, we elucidate the interplay between the drive and the pinning which can conspire to make the path-dependent AC-susceptibility response of different metastable vortex states appear identical. An optimal balance between the pinning and driving force is needed to view the metastability effects in typically weakly pinned specimens of low temperature superconductors. As one uses samples with larger pinning in order to differentiate the response of different metastable vortex states, one encounters a new phenomenon, viz., the second magnetization peak (SMP) anomaly prior to the PE. Supercooling/superheating can occur across both the PE and the SMP anomalies and both of these are known to display non-linear characteristics as well. Interplay between the path dependence in the critical current density and the non-linearity in the electromagnetic response determine the metastability effects seen in the first and the third harmonic response of the AC susceptibility across the temperature regions of the SMP and the PE. The limiting temperature above which metastability effects cease can be conveniently located in the third harmonic data, and the observed behavior can be rationalized within the Bean’s critical state model. A vortex phase diagram showing different vortex phases for a typically weakly pinned specimen has been constructed via the AC susceptibility data in a crystal of 2H-NbSe₂ which shows the SMP and the PE anomalies. The phase space of coexisting weaker and stronger pinned regions has been identified. It can be bifurcated into two parts, where the order and disorder dominate, respectively. The former part continuously connects to the reentrant disordered vortex phase pertaining to the small bundle pinning regime, where the vortices are far apart, interaction effects are weak and the polycrystalline form of flux line lattice prevails.

Keywords. Peak effect; second magnetization peak; order-disorder transition; vortex phases; metastability; spinodal line.

PACS Nos **74.25.Qt; 64.70.Dv; 74.25.Dw; 74.25.Sv**

1. Introduction

The richness of the phenomenon of the peak effect (PE) in the mixed state of Type-II superconductors has engrossed the vortex physics community for over forty years [1–5]. The ubiquitous PE phenomenon is an anomalous enhancement in the critical current density (J_c) of a superconductor as a function of applied field or temperature in the vicinity of the superconducting to the normal state transition [1,2]. The vortex matter can be viewed as an elastic medium in a random pinning environment along with the influence of thermal fluctuations acting on the pinned vortices. According to a heuristic argument due to Pippard [6] and subsequent theoretical work by Larkin and Ovchinnikov [7], the PE is considered to be triggered by an incipient softening of the elastic vortex lattice as the normal state is approached. The softer lattice presumably gets conformed to its pinning environment more snugly, thereby producing an enhancement in the pinning (or J_c). The notion that the PE can be associated with an inevitable and eventual softening of the vortex lattice encouraged widespread belief that the PE is a (precursor) signature of the phenomenon of flux line lattice (FLL) melting [8,9]. It is useful to recall at this juncture that FLL melting phenomenon has been unambiguously verified only in the anisotropic high temperature cuprate superconductors (HTSC) [10]. The PE phenomenon has, however, been widely studied in low T_c superconductors (LTSC) as well as in the HTSC. In the LTSC, the smallness of the Ginzburg number, which measures the relative importance of thermal fluctuations *vis-à-vis* superconducting condensation energy, makes the thermally driven FLL melting line lie very close to the $H_{c2}(T)$ line [3]. The investigations in a variety of samples of LTSC reveal that the anomalous behavior pertaining to the PE could surface up sufficiently below the $H_{c2}(T)/T_c(H)$ values and the separation between the onset position of the PE anomaly and $T_c(H)$ line correlates well with the level of effective disorder in the sample [11]. Such observations seem to suggest that, generically, the PE as a phenomenon needs a clarification and distinction from the pristine thermally driven FLL melting transition.

In any realistic sample of a Type-II superconductor, the inevitable presence of residual quenched random disorder is anticipated to compromise the perfect translational symmetry of the Abrikosov flux line lattice state. However, it was argued by Larkin and Ovchinnikov (LO) [12] that in the presence of pinning, the spatial order in the vortex matter could survive within a domain having dimensions much larger than the intervortex spacing, but smaller than the typical sample size. In recent times, Giamarchi and Le Doussal [13] have shown that the spatial correlations in the weakly pinned vortex matter could decay much more slowly, in an algebraic manner, such that a good positional and high orientational order, equivalent to a quasi-long range order (notionally a ‘Bragg glass’ state), can be observed over length scales comparable to the sample dimensions. A contemporary view that has gained

Effect of pinning and driving force on metastability effects

acceptance about the PE anomaly is that it represents a transition from a weakly pinned Bragg glass state to a stronger pinned multi (or micro) domain vortex glass state. Bulk AC susceptibility studies in a very weakly (nascent) pinned superconducting specimen of 2H-NbSe₂ had pointed towards the association of the PE with the first-order nature of the underlying transition in the pinned vortex matter [14]. Eventually, the local AC susceptibility measurements by scanning micro-Hall bar microscopy [4] in the typically weakly pinned single crystals of 2H-NbSe₂ directly elucidated the presence of an interface separating the weaker and stronger pinned regions across the peak effect region, thereby endorsing its first-order nature and the associated metastability effects.

The presence of a first-order transition line in the magnetic phase (H, T) diagram of a weakly pinned superconductor imbibes in it the notion of supercooling and superheating effects across it [15–17]. An STM imaging study [18] along with an analysis of the instantaneous positions of the individual vortices in a very weakly pinned crystal of 2H-NbSe₂ led to the surmise that neighboring vortices execute collective motion below the onset temperature of the PE, which transforms to positional fluctuations (random excursions) of individual vortices above it. A small angle neutron scattering (SANS) study [19] in a typically weakly pinned crystal of Nb could reveal the superheating of the ordered Bragg glass phase above the onset temperature of the PE along with the usual supercooling of the disordered vortex glass phase below it. An elucidation of the superheating effects across the PE in a variety of single crystals of 2H-NbSe₂ by bulk transport measurements using a fast current ramp procedure [20] has resulted in the demarcation of a generic spinodal line corresponding to the limit of the superheating of the ordered state. Above the spinodal line, the threshold force needed to depin and drive the lattice (i.e., critical current density J_c) is independent of the thermomagnetic history of the underlying pinned vortex matter.

The work of Xiao *et al* [20] on the spinodal line in conjunction with the correlation between the effective disorder, the structure across the PE and the metastability effects [14,17,21] raises an issue relating to the possible connection between the quenched random disorder and the details characterizing the spinodal nature. In the present report, we shall focus on the results pertaining to this issue. It had been shown earlier [14,17,21] that with the gradual enhancement in the quenched random pinning, the first-order nature of the order–disorder transition associated with the PE is not severely compromised; only the process of disordering starts to comprise several distinct steps. In a nascent pinned sample [14], the interface separating the weaker and stronger pinned regions is perhaps very fragile, and the metastability effects in such a sample get wiped out easily by an infinitesimally small driving force. In typically weakly pinned specimen of LTSC systems (like, Nb crystal used in SANS experiment [19], or the 2H-NbSe₂ crystals used in micro-Hall bar microscopy [4]), the metastable states are more robust and the thermomagnetic history effects can be conveniently probed via contactless AC susceptibility measurements, with a minimal level of an AC driving force. By performing broad-band noise measurements in the in-phase AC susceptibility (χ'_ω) and the third harmonic ($\chi'_{3\omega}$) measurements, one can demarcate the limits of metastability and determine the spinodal line in the vortex phase diagram. We elucidate the above-stated behavior in the samples of two very different superconducting compounds [21], viz.,

2H-NbSe₂ ($T_c \sim 6$ K) and CeRu₂ ($T_c \sim 6.3$ K) to establish the generic nature of the spinodal line, so determined.

2. Experimental

The AC susceptibility studies have been carried out using a conventional double coil arrangement affixed coaxially inside a superconducting magnetic coil and employing a mutual inductance bridge [22]. Most of the data have been recorded in the frequency interval of 21 Hz to 211 Hz and with an AC amplitude (h_{AC}) lying in the range of 0.5 Oe to 3.5 Oe (r.m.s.). The samples studied include the crystals X, Y', Y, Z and Z' of 2H-NbSe₂ [14,17,23] and a single crystal of CeRu₂ [21]. The crystal X of 2H-NbSe₂ is the most weakly pinned sample, with a $T_c(0) = 7.225$ K, the crystals Y' and Y are somewhat strongly pinned than the crystal X with $T_c(0) = 7.25$ K and 7.17 K, respectively. The crystals Z and Z' have $T_c(0)$ values in the neighborhood of ~ 6 K and they probably contain few hundred ppm of Fe impurity in them [21]. From the sample X to Z' , the J_c values at 4.2 K in the low field region (~ 1 kOe) vary from about 10 A/cm² to 10³ A/cm² [23]. We reckon that the FLL correlations in the vortex matter in the crystals Z and Z' of 2H-NbSe₂ are like those in the typically weakly pinned crystals of other low T_c superconducting compounds, e.g., CeRu₂, Ca₃Rh₄Sn₁₃, etc. [21,24].

3. Results and discussions

3.1 AC susceptibility measurements in the crystals of 2H-NbSe₂ with varying pinning

Figure 1 shows the in-phase AC susceptibility response, χ'_ω , in the different crystals X, Y', Y, Z and Z' of 2H-NbSe₂ in a field of 15 kOe. The AC susceptibility response varies as [25], $\chi'_\omega \sim -1 + \alpha h_{AC}/J_c$, where α is a geometry- and size-dependent factor. This implies that the χ'_ω response closely mimics the behavior of J_c in the sample. In different samples, we compare the J_c values of the vortex states corresponding to different thermomagnetic histories, viz., the zero-field-cooled (ZFC) state and the two field-cooled (FC) modes. The response of a FC state is first measured while cooling down (FCC), and later measured while warming up (FCW).

Figure 1a shows the χ'_ω response in the cleanest crystal X for the vortex states in the ZFC, FCC and FCW modes. All the three responses are observed to overlap, such that no distinction can be made amongst them. In this crystal, we find the PE to be a very sharp feature (which occurs over a width of 20–40 mK or so). Considering that the crystal X has the least amount of disorder, one may argue that the properties of the first-order nature of the PE transition should get best exemplified in this crystal. It was, therefore, expected that a substantial hysteresis in the χ'_ω responses should have been evident between the ZFC and the FCC states due to the possible supercooling effect below the onset temperature of the first-order transition. While the data shown in figure 1a for the vortex states in a field of 15 kOe is a representative one for the crystal X , we found the absence of any thermomagnetic history dependence in the χ'_ω response (i.e., differences between

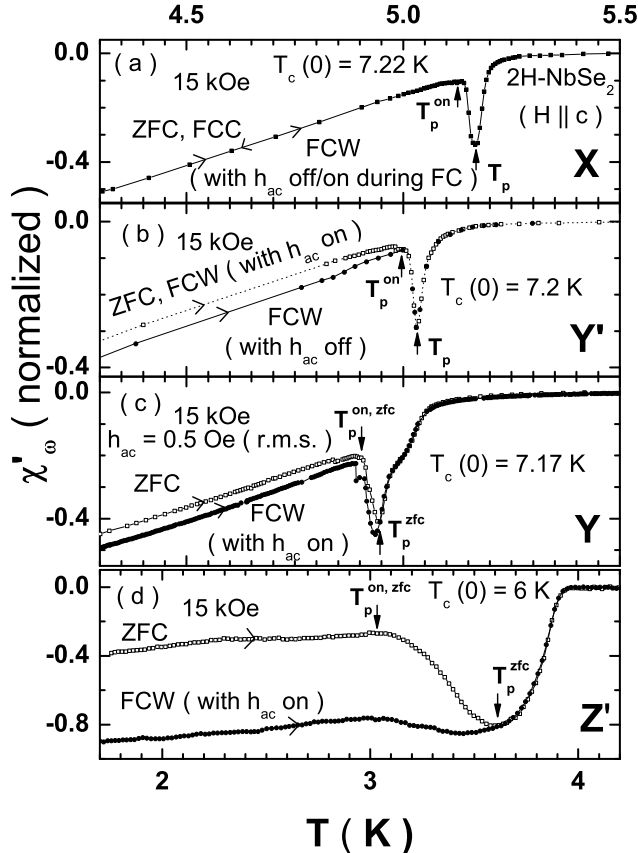


Figure 1. In-phase AC susceptibility data showing peak effect (PE) in a field of 15 kOe with different thermomagnetic histories in single crystals of 2H-NbSe₂. The crystals X, Y', Y and Z' have progressively enhanced pinning. The crystal Z' has a lower $T_c(0)$ value of ~ 6 K as it presumably contains 200 ppm of Fe impurity. Panel (a) shows that in the most weakly pinned crystal X, all the three responses, ZFC, FCC, FCW (recorded after h_{AC} ON or OFF during field-cooling) are identical. In panel (b), the two FCW responses (with h_{AC} ON and OFF during field-cooling) in the crystal Y' are different. While the former coincides with ZFC (dotted curve), the latter overlaps with FCC (the solid line). The panel (c) shows that in the crystal Y, the χ'_{ω} response in the FCW with h_{AC} ON differs from that in the ZFC state. In the panel (d), the χ'_{ω} data in the crystal Z' is such that the FCW response represents the supercooling of the vortex state existing at the peak position of the peak effect. The onset (T_p^{on}) and peak (T_p^{ZFC}) temperatures of the PE in the ZFC mode have been identified in each of the panels.

the ZFC and the FCC or the FCW states) across the PE transition at all magnetic fields in this sample (all data not being shown here). A possible reason for the absence of the hysteresis between the ZFC and the FC states in the sample X is

a subtle effect of the superimposed AC magnetic field h_{AC} . We elucidate next an additional facet of h_{AC} in the AC susceptibility measurements on the pinned vortex matter, which is different from its obvious role in measuring the shielding response from the macroscopic screening currents induced by its imposition on the sample.

Figure 1b displays the χ'_ω response of the vortex state with two different thermomagnetic histories, viz., the ZFC and the FCW, in the crystal Y' at 15 kOe. We observe that the sharpness of the PE in this crystal is comparable to that in crystal X , but the response of the ZFC and FC vortex states can be made to differ, unlike the situation observed in the crystal X . We find that for the ZFC and FCW modes, the χ'_ω responses in the crystal Y' coincide if h_{AC} is kept ON while the sample is initially cooled down in a DC magnetic field to the lowest temperature (which was 4.3 K in the present case). Such a situation is identical to that in the sample X . However, if the sample Y' is field-cooled with h_{AC} switched off during the cooling, and it is switched on only when one begins the FCW measurement, then one observes a measurable difference in the ZFC and the FCW responses. This behavior is indeed different from that observed in the crystal X . These imply that depending on the pinning in the sample, h_{AC} has the potential to modify the path dependence in J_c . Such an attribute becomes further exemplified as we examine the results on the samples with higher pinning, viz., the crystals Y and Z' . In these samples, it is significant to note that the differences in the responses of the ZFC and the FCW states survive, whether h_{AC} is kept ON or OFF during the initial field-cooling procedures (see figures 1c and 1d). *Note that the limiting temperature below which the χ'_ω response exhibits thermomagnetic history dependence (cf. the positions of arrows marked in the different panels of figure 1) could be a function of h_{AC} and the extent of effective pinning in the sample.* To emphasize another observation, the notional peak position of the PE in the ZFC (or the FCW) mode does not necessarily mark the limiting temperature above which the thermomagnetic history effects in the χ'_ω response cease.

From the χ'_ω responses in figures 1c and 1d, it is evident that $J_c^{\text{ZFC}} < J_c^{\text{FCW}}$. To understand the behavior of J_c corresponding to the vortex states with different thermomagnetic histories, we take recourse to a contemporary view [4] that in the PE region the vortex state comprises *an admixed inhomogeneous phase*, with the coexistence of ordered and disordered regions. The ZFC state prior to the PE represents an ordered weakly pinned state, which is characterized by a low J_c value. The FCW state on the other hand could correspond to the phase above the peak temperature, viz., a predominantly disordered, strongly pinned vortex state that can get supercooled down to the low temperatures during field cooling. The FCW state, therefore, carries a higher J_c value. We have elucidated through the results in figure 1b that the non-observation of metastable phases in the χ'_ω response need not imply the absence of path dependence in J_c .

In the presence of very weak pinning, the metastable states of the vortex matter could be very fragile. Any attempt to couple the system to the external environment perturbs the underlying vortex matter such that it is driven into a different state, thereby masking (i.e., altering) the pristine information pertaining to the metastability. The process of keeping h_{AC} switched ‘ON’ during field cooling the vortex matter can also help the disordered regions in exploring the possibilities of transformation into the ordered regions of the ZFC mode. This is best exemplified

Effect of pinning and driving force on metastability effects

by the data in figure 1a, wherein in the crystal X , the χ'_ω response is identical, irrespective of whether h_{AC} was kept ‘ON’ or ‘OFF’ during initial field cooling. In the sample X , even while h_{AC} was kept OFF during FC, the application of a small h_{AC} to measure the χ'_ω response during the FCW mode resulted in driving the field-cooled state towards the ordered state of the ZFC mode.

In the sample Y' , where the pinning is somewhat stronger than that in sample X , the option of keeping the h_{AC} switched ON/OFF during the initial field-cooled procedure demonstrates the competition between progressive enhancement in pinning and the annealing effect of h_{AC} . The enhanced pinning in sample Y' arrests the hysteresis across the PE and allows the difference between the ZFC and the FCW state to be observed clearly before the onset temperature of the peak effect (T_p^{on}). The inevitable dynamical changes which accompany the PE phenomenon make the χ'_ω responses for the ZFC and the FCW states nearly identical for $T > T_p^{on}$ in the sample Y' . The progressive increase in pinning can therefore aid the metastability of the super-cooled (FC) phase against the thermal fluctuations and the possible perturbations from h_{AC} . To search for the true location, where the path dependence in J_c ceases, in other words, to determine the spinodal temperature (T^*) which is not influenced by the driving forces, one needs to resort to a sample with optimal pinning. *Therefore, to generate metastability in the vortex matter and to sustain its imprint in a measurement, one requires a crucial balance between the strength of the driving force ($h_{AC}/transport current$), disorder/pinning and the temperature.* At this juncture, it may also be pertinent to recall and compare the results of the electrical transport data of Xiao *et al* [26] in a crystal of 2H-NbSe₂ with χ'_ω response as in our samples Y and Y' . It has been reported that the transport J_c value for the FC state in a very weakly pinned specimen differs from that in the ZFC state only during the first ramp-up of the current while recording the I -V data. The J_c values determined during the ramp-down cycle or during the subsequent ramp-up cycles were found to be equal to that for the ZFC state. The passage of transport current presumably reorganizes the disordered state of the FC mode towards the ordered ZFC mode, when the pinning effects are in the nascent stage. Xiao *et al* [20] had to later adopt the procedure of fast current ramp to explore the metastable states above the notional onset temperature of the PE. They found that the superheating of the ordered state could be observed up to a limiting temperature T^* , which exceeds the notional peak temperature of the PE for the vortex state prepared in the ZFC mode [20].

The plots in figure 1d appear to imply that the metastability effects in the χ'_ω response would cease above the peak temperature T_p , as was conventionally believed [9,27,28]. The FC state in this sample can be ascribed to freezing in of the disordered vortex state at the peak position of the PE, where the lattice was believed to be homogeneously amorphous [21,28]. However, recent work by Xiao *et al* [20] desires a serious revision of the above presumption. A transformation that sets in at T_p^{on} results in an admixed state of ordered and disordered phases. Both these fractions carry different J_c values and possess different temperature dependences. As the temperature increases from T_p^{on} towards T_p , the fraction of the ordered vortex phase decreases and that of the disordered phase increases, and correspondingly the observed J_c value also increases. The relative fractions of these two phases and their temperature dependences determine the peak position (i.e., T_p/H_p) of the

PE anomaly. In view of this, the relationship, if any, between T_p and the limiting temperature at which the metastability effects cease is not very apparent. We have set out to clarify this issue via the AC susceptibility measurements.

3.2 Comparison of AC susceptibility data in the crystals of 2H-NbSe₂ and CeRu₂

As stated earlier, in order to study the features associated with a first-order transition one should in principle attempt to select a sample with the least amount of disorder. However, the data in figure 1 show that to study features related to the spinodal temperature T^* via the AC susceptibility measurements, we were compelled to choose the samples of Z and Z' category, which have significantly higher level of disorder than the sample X . While it is clear that with an enhanced pinning, the metastability features of the vortex matter stand preserved, it is not however apparent as to whether the first-order character of the PE transition stands retained at comparatively higher levels of disorder. A trend which emerges from the χ'_ω response in figures 1a to 1d, is that between T_p^{on} and T_p , the PE phenomenon undergoes a broadening with progressive increase in the effective pinning. It could be argued that this indicates that a sharp first-order-like PE transition is being transformed into a continuous transition. However, in this context, it is useful to recall that a novel notion of (multi-step) fracturing had been demonstrated earlier [21,24]. The first-order nature of the PE transition is not destroyed in samples with higher pinning, it only transforms into multiple small first-order-like jumps, which comprise the notion of fracturing.

Figure 2 shows a comparison of the AC susceptibility response at different AC amplitudes in a crystal Z of 2H-NbSe₂ with that in a crystal of CeRu₂ (cubic system with $T_c(0) \approx 6.3$ K), with a level of pinning comparable to that in crystal Z [21]. In both these samples, we observe in figures 2a and 2c that although the PE is a broad feature, yet it is characterized by multiple sharp jumps commencing at T_p^{on} in the $\chi'_\omega(T)$ response, characterizing the fracturing transition. A well-ordered vortex phase is considered to transform into a multi-domain-like state, with pockets of ordered and disordered regions created, possibly via the progressive permeation of topological defects like dislocations, into the ordered vortex phase. At each first-order-like jump, some particular pockets with a collection of well-ordered vortices (with a pocket characterized by a low J_c value), transform into a disordered phase with a higher value of J_c , locally. As the number of such domains increases, with intervening disordered vortex phase, the average J_c of the sample increases leading to a PE-like feature above T_p^{on} . The coexisting ordered and disordered phases are not nucleated by merely supercooling the vortex matter below a first-order transition, they can also get generated due to the staggered nature of the first-order transition as a consequence of the fracturing phenomenon. The fraction of domains with disordered vortices is larger while field-cooling below the fracturing transition, and this result in prominence of the metastability effect.

The above description finds an echo in the plots contained in figures 2b and 2d. We observe that in the samples of 2H-NbSe₂ and CeRu₂, there is a substantial difference between the ZFC and the FCW states for $h_{\text{AC}} = 0.5$ Oe (figures 2a and 2c). For larger h_{AC} values (i.e., between 2 Oe and 3.5 Oe, as shown in the plots for

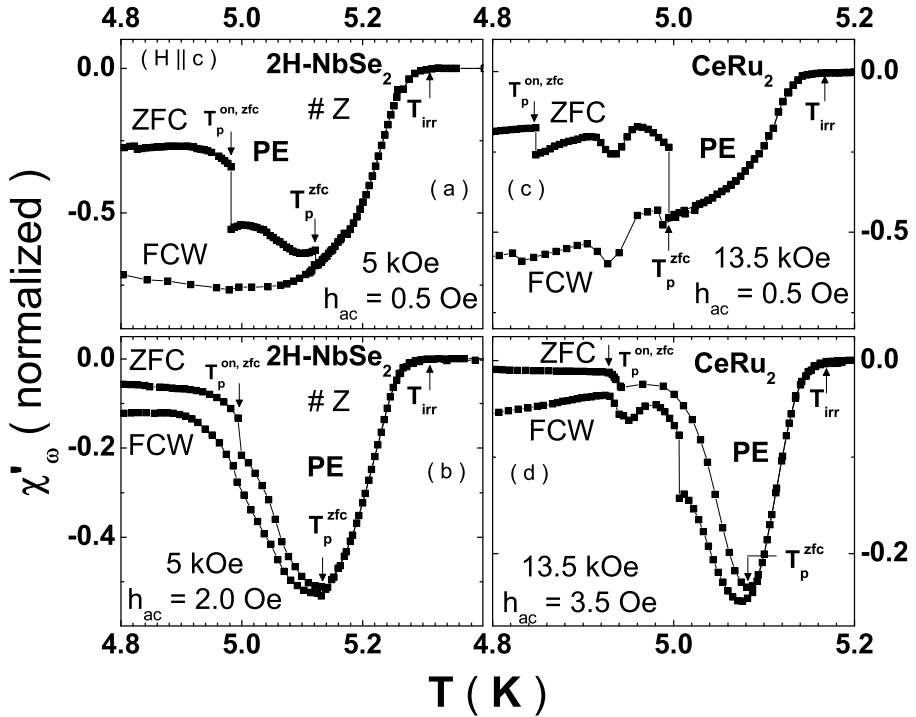


Figure 2. Comparison of the χ'_ω data at the fields indicated in the ZFC and the FCW modes with different amplitudes of the AC driving force (h_{AC}) in a typically weakly pinned single crystal Z of 2H-NbSe₂ ($T_c(0) \approx 6.0$ K) and in a crystal of CeRu₂ ($T_c(0) \approx 6.3$ K). The positions of the onset and peak temperatures have been identified in each of the panels.

figures 2b and 2d), the PE becomes a narrower transition and the fracturing features can get suppressed and, consequently the metastability response (as reflected by the differences between the ZFC and FCW responses) also stands reduced. The connection between the weakening of the fracturing transition and the decrease in metastability is presumably related to the annealing effect of the h_{AC} drive in modifying the relative fractions of the ordered and disordered regions between T_p^{on} and T_p . With a larger h_{AC} drive used for χ'_ω measurements, the residual disordered pockets in the ordered vortex matter get transformed into the ordered ones, prior to the onset of the PE. The vortex matter thus approaches a single domain-like picture of the ordered vortices as in the samples X and Y' of 2H-NbSe₂, which then undergoes a sharp PE transition, rather than a multi-step fracturing transition. It is also pertinent to note that with the enhancement in the ordered fraction of vortices in the presence of a driving force, the disordered domains of vortices can permeate and survive in the midst of the ordered vortex matter only at relatively higher temperature (cf. the T_p^{on} and T_p values in figures 2b and 2d with those in figures 2a and 2c, respectively). It is also instructive to compare FCW responses in figures 2a and 2c with those in figures 2b and 2d, respectively. The supercooled state in the FCW mode need not undergo order-disorder transition across the PE region; such a

behavior is evident when h_{AC} is small (cf. figures 2a and 2c). However, a larger h_{AC} drive can reorganize the initial FCC state during warm-up and eventually depict an order-disorder transition across the temperature region of PE, as is evident in figures 2b and 2d.

Having explained the metastability features associated with the fracturing transition seen in samples with higher pinning, and determining the optimum range of parameters for h_{AC} , disorder and temperature, we now dwell on the demarcation of the limit of metastability in the vortex phase diagram. Figure 3 shows the $\chi'_\omega(T)$ response at different applied fields for ZFC, FCC and FCW modes in sample Z' of 2H-NbSe₂. Note that at the lowest temperature, the FCW and FCC responses are identical, at higher temperatures the FCW state is more ordered in comparison to the FCC state. Apart from the behavior of metastability and the PE, we observe an additional anomaly in the behavior of the χ'_ω response on the ZFC branch. In samples having a level of pinning as in the crystal Z' , we can see the occurrence of an anomalous enhancement in J_c deep in the mixed state beginning at T_{SMP}^{on} , corresponding to the second magnetization peak (SMP) feature observed in the isothermal magnetization hysteresis ($M-H$) loops well before the onset of the usual PE at T_p^{on} [29]. The SMP feature is different from the fracturing phenomenon which gets triggered at (or near) T_p^{on} (see figure 3a). It suffices to recall and state here that the (two) anomalies of the SMP and the PE are distinct and different [29]. It may be worthwhile now to ask as to at what stage does the phase coexistence of ordered and disordered phase commence, in the presence of a SMP anomaly. A conventional notion as alluded to in the description earlier would imply that the phase coexistence region commenced from the onset position of the PE. We shall now show that such a notion desires a revision in view of the data presented in the panels of figure 3. Closely associated with the notion of phase coexistence and the first-order nature of the PE is that of the metastability.

While examining the metastability response, it is instructive to focus on the interesting behavior illustrated in the data recorded at 6 kOe (cf. figure 3b). Note that the peak temperature of the PE is different for different thermomagnetic histories, the highest value being in the ZFC state, T_p^{ZFC} . Similar trend can be noted at other magnetic fields (cf. figures 3c and 3d). Such a behavior for the χ'_ω response for the vortex states with different thermomagnetic histories, is analogous to that reported for the transport critical current $I_c(T)$ data in a crystal of 2H-NbSe₂ by Xiao *et al* (see figure 1 of ref. [20]). Vortex states with different histories are characterized by the different fractions of the ordered and disordered phases. The observation that $T_p^{\text{FCC}} < T_p^{\text{FCW}} < T_p^{\text{ZFC}}$ implies that the limiting temperature at which the sample is homogeneously filled with the disordered phase does not lie in the temperature interval, from T_p^{FCC} to T_p^{ZFC} .

The $\chi'_\omega(T)$ response for a given H is essentially dictated by $J_c(T)$. The temperature above which $\chi'_\omega(T)$ (or, $J_c(T)$) becomes independent of the thermomagnetic history of the specimen appears to lie even above the (highest) peak temperature, i.e., at $T > T_p^{\text{ZFC}}$. Figure 4a focuses attention onto the plots showing $(\chi'_\omega^{\text{ZFC}} - \chi'_\omega^{\text{FCW}})$ and $(\chi'_\omega^{\text{ZFC}} - \chi'_\omega^{\text{FCC}})$ at 12 kOe in the sample Z' . In this panel one can identify the limiting temperature T^* above which the χ'_ω response becomes path independent, viz., where the differences $(\chi'_\omega^{\text{ZFC}} - \chi'_\omega^{\text{FCW}})$ and $(\chi'_\omega^{\text{ZFC}} - \chi'_\omega^{\text{FCC}})$ vanish. In the sample Z' , due to the relatively strong pinning and the fracturing

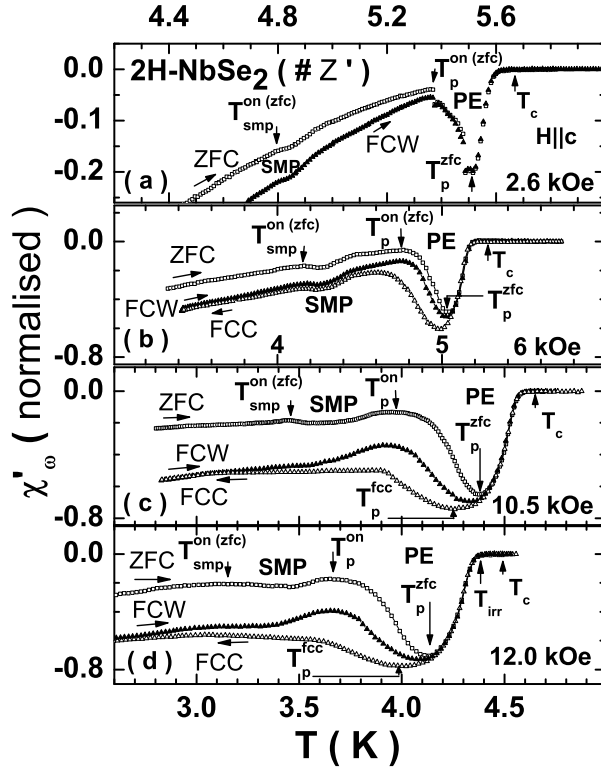


Figure 3. χ'_ω data at different applied fields for different thermomagnetic histories in a crystal Z' ($T_c(0) \approx 6.0$ K) of 2H-NbSe₂. Note the occurrence of two anomalous variations corresponding to the SMP and the PE in each of the panels. The $\chi'_\omega(T)$ curves at $H = 2.6$ kOe in the panel (a) display the notion of step-wise fracturing across the PE, as in figure 2a for the sample Z at 5 kOe. The onset temperature of the SMP and the PE and the peak position of the PE in the ZFC mode have been marked in all the panels.

phenomenon, the determination of the limit of metastability effects is insensitive to perturbations from h_{AC} . We believe that the above procedure yields a reasonable estimate of the spinodal temperature, T^* , for 2H-NbSe₂ samples with J_c (~ 1 kOe, 4.2 K) ≥ 1000 Amps/cm². However, the above procedure may not suffice for all weakly pinned samples, like, the crystals X and Y' of 2H-NbSe₂. It is therefore desirable to explore an alternative way to determine the value of T^* .

3.3 Spinodal temperature T^* and the third harmonic AC susceptibility measurements

The critical state model (CSM) relates the macroscopic J_c to the hysteretic magnetization response of a superconductor [30,31]. It is well-documented [32–36] that new features get added to the pristine relationship between $J_c(H)$ and the

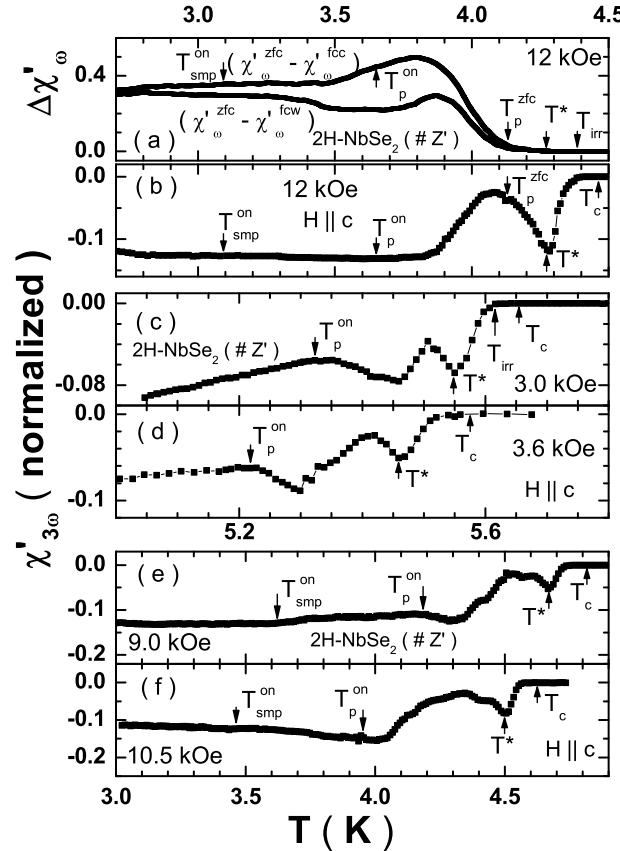


Figure 4. The panels (a) and (b) show the plots of difference susceptibility $\Delta\chi'_\omega$, i.e., $(\chi'^{\text{ZFC}}_\omega - \chi'^{\text{FCC}}_\omega)$ and $(\chi'^{\text{ZFC}}_\omega - \chi'^{\text{FCW}}_\omega)$, and the third harmonic signal $\chi'_3\omega$ in a field of 12 kOe ($H \parallel c$) in the crystal Z' of 2H-NbSe₂. The positions of $T_{\text{SMP}}^{\text{on}}$, T_p^{on} and T_p for the ZFC mode, as evident from the curve in figure 3d, have been identified in these two panels. T^* in the panel (a) identifies the temperature at which the difference $(\chi'^{\text{ZFC}}_\omega - \chi'^{\text{FCC}}_\omega)$ vanishes and merges into the baseline. This value of T^* is then marked in panel (b). Note that $\chi'_3\omega$ response shows a monotonic decrease at $T > T^*$. The panels (c) to (f) show $\chi'_3\omega$ curves at different applied fields with $h_{\text{AC}} = 2.5$ Oe (r.m.s.) in the crystal Z' of 2H-NbSe₂. The respective T^* values have been identified in these panels. It is apparent that the $\chi'_3\omega$ collapses above T^* and merges into the baseline as $T \rightarrow T_{\text{irr}} (< T_c)$, where T_{irr} is the notional irreversibility temperature for a given h_{AC} and the frequency value in which the AC susceptibility measurements stand performed.

magnetization hysteresis, when $J_c(H)$ does not remain single-valued function of H . For instance, the minor hysteresis loops can display anomalous characteristics, like, an asymmetric shape [34,35], excursions beyond the envelope $M-H$ loop [36], etc., when $J_c(H)$ turns path dependent. In the back drop of these observations, it is

Effect of pinning and driving force on metastability effects

instructive to examine the response of the third harmonic of the AC susceptibility across the SMP and PE regions, i.e., from below the onset temperature of the first of the two anomalous variations in J_c up to the irreversibility temperature (T_{irr}), where the (bulk) J_c ceases. To be specific, consider the cool down of a weakly pinned Type-II superconducting sample from above a given $T_c(H)$ value to below its $T_{\text{irr}}(H)$, where the finiteness of J_c would result in a non-linear magnetization response which could generate a measurable third harmonic signal in the AC susceptibility measurements. Such a third harmonic signal would be expected to follow the increase in $J_c(T)$ for a given H as $(T_{\text{irr}} - T)$ increases, as per a prescription of the CSM for path independent $J_c(H, T)$ [30,31]. The onset of the history dependence in $J_c(H)$ could compromise the above-stated notion, arising from the applicability of the CSM. Below T^* , due to the onset of the path dependence in J_c , qualitative changes could occur in the behavior of the non-linear response at the nucleation of an inhomogeneous phase.

The plots in figures 4b to 4f explore the limit of the path dependence in $J_c(H)$ via the study of the temperature dependence of the third harmonic AC susceptibility data, $\chi'_{3\omega}$, in the sample Z' of 2H-NbSe₂. In figure 4b, we draw attention specifically to the behavior of $\chi'_{3\omega}$ just above T^* . Warming up from the low temperature side, as the temperature crosses the limit T^* , $\chi'_{3\omega}(T)$ is seen to monotonically decrease and eventually vanish at the irreversibility temperature, T_{irr} ($< T_c(H)$). There does not appear any simple correspondence between $\chi'_{\omega}(T)$ and $\chi'_{3\omega}(T)$ for $T_{\text{SMP}}^{\text{on}} < T < T^*$ (cf. figures 3d and 4b). Figure 3d shows that $\chi'_{\omega}(T)$ monotonically decreases above T_p^{ZFC} , reflecting the collapse in J_c above the peak position of the PE. The $\chi'_{3\omega}(T)$, on the other hand in figure 4b, appears to enhance between T_p^{ZFC} and T^* . The $\chi'_{3\omega}(T)$ response is seen to turn around only above T^* , and follow $J_c(T)$ thereafter. Thus, the onset of an inhomogeneous phase at $T < T^*$ produces modulations in the behavior of non-linearity or in the $\chi'_{3\omega}$ response.

To establish the assertion on the imprint of the limit of the path independence in J_c in the $\chi'_{3\omega}(T)$ data, we can examine the above-stated behavior at different fields in figures 4c to 4f, and note the one-to-one correlation between the values of T^* determined from $\chi'_{\omega}(T)$ data in different thermomagnetic histories and the limiting temperatures above which $\chi'_{3\omega}(T)$ monotonically decreases. The T_p^{on} , T_p^{ZFC} and T^* values have been marked for each of the curves in figure 4. At $T < T^*$, the modulations in $\chi'_{3\omega}(T)$ display complex behavior, dictated by the (intrinsic) changes in the relative fraction of the ordered and disordered phases (path dependence in $J_c(T)$) and the additional changes induced by the h_{AC} value in which the $\chi'_{3\omega}(T)$ data are recorded. The T^* , however, does not appear to vary in any noticeable manner with the amplitude of h_{AC} (all data not shown here). It is also worthwhile to note that the modulation in the $\chi'_{3\omega}(T)$ signal ceases close to $T_{\text{SMP}}^{\text{on}}$. In fact, if we approach $T_{\text{SMP}}^{\text{on}}$ from the lower temperature side, the $\chi'_{3\omega}(T)$ plots appear to show an enhancement in the non-linear response at $T > T_{\text{SMP}}^{\text{on}}$. Such an observation would get rationalized by invoking the notion that the SMP and the PE are non-linear phenomena [9]. In the absence of complications induced by (possible) phase-coexistence and history effects, $\chi'_{3\omega}(T)$ would have been expected to follow the modulation as displayed by $\chi'_{\omega}(T)$. We believe that the possibility of phase-coexistence commences at $T_{\text{SMP}}^{\text{on}}$ and lasts up to T^* .

3.4 Correlation between $\chi'_{3\omega}(T)$ and measurement of noise in $\chi'_\omega(T)$

To further substantiate that the values of T^* determined from the $\chi'_{3\omega}$ response indeed physically correspond to the spinodal temperatures, we explore the correlation between the $\chi'_{3\omega}(T)$ and the noise signal in $\chi'_\omega(T)$ [21], which can be easily recorded using a lock-in amplifier having a wide band filter option. The above-stated noise signal is believed to measure the fluctuations in $\chi'_\omega(T)$ and it is argued [21] to reflect the possibility of transformations amongst metastable states accessible from a given mode (ZFC/FC).

Figure 5 depicts the plots of $\chi'^{\text{ZFC}}_{3\omega}(T)$ in $h_{\text{AC}} = 3.5$ Oe (r.m.s.) and the noise in $\chi'^{\text{ZFC}}_\omega(T)$ in $h_{\text{AC}} = 0.5$ Oe (r.m.s.) in a field of 5 kOe in the sample Z of 2H-NbSe₂ and in field of 13.5 kOe CeRu₂ crystal. In different panels of figure 5, we have marked the respective values of T^* as determined from the onset of non-monotonic modulations in $\chi'_{3\omega}$ response. In view of the notion of the existence of a homogeneously disordered phase above T^* , it is indeed not a coincidence that the noise signals in panels (b) and (d) of figure 5 recede to the background value as $T \rightarrow T^*$. Taking cue from earlier studies of noise in transport experiments [37,38], Banerjee *et al* [21] had argued that the increase in noise at $T = T_p^{\text{on}}$ (equivalent to the temperature of the onset of plastic flow, T_{pl} , in ref. [21]) reflects the possibility of enhancement in transformations amongst the coexisting [4] metastable states in a fractured (partially disordered) vortex solid (which exists at $T < T^*$). The setting in of the decrease in the noise signal as $T \rightarrow T_p$ was considered to imply the effect of phase cancellation of a large number of incoherent fluctuations as the vortex matter moves towards the fully disordered state. In such a framework, the possibility of coexistence of ordered pockets embedded in the disordered medium would cease as $T \rightarrow T^*$, and the noise signal would be expected to recede to the background value. In the context of our present results, the $T^*(H)$ values indeed represent the notion of the spinodal line, $T_s(H)$ [20,39].

3.5 Magnetic phase diagram in a typically weakly pinned crystal of 2H-NbSe₂

To comprehend a variety of results presented above, we have constructed a field-temperature (H, T) diagram for the sample Z' of 2H-NbSe₂ in figure 6. It includes the values of the onset temperatures of the SMP and the PE anomalies, along with the values of T_p^{ZFC} , $T^*(H)$, $T_c(H)$ and $H_{\text{plateau}}(T)$. In sample Z' (or Z), there is adequate perceptible difference in T_p^{ZFC} and $T^*(H)$, and this difference enhances as H increases. However, in the samples Y and Y' of 2H-NbSe₂, where the PE manifests as a sharp transition, T^* values lie in very close proximity of the corresponding peak temperature values. In the vortex phase diagram of figure 6, the plateau line, $H_{\text{plateau}}(T)$, passes through the limiting fields [11,17] below which the collective pinning regime gives way to the small bundle pinning regime. It seems appropriate to identify the (H, T) space between the $H_{\text{plateau}}(T)$ and the $T_{\text{SMP}}^{\text{on}}(H)$ as the Bragg (elastic) glass region [13]. Above the $T^*(H)$ line, where the metastability effects cease, the vortex matter exists in the pinned amorphous phase. The phase diagram demarcates the regime of phase-coexistence [40]. We

Effect of pinning and driving force on metastability effects

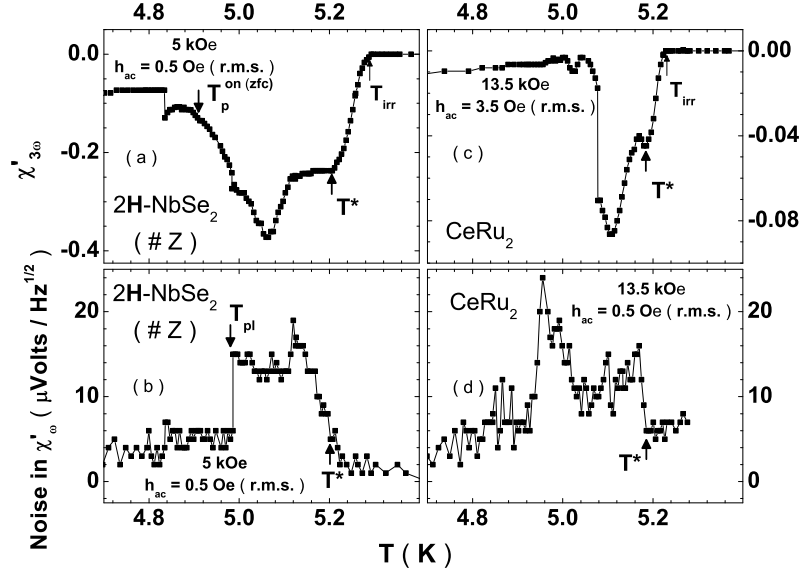


Figure 5. A comparison of third harmonic, $\chi'_{3\omega}$ response and the noise signal in the AC susceptibility at the fields indicated in the typically weakly pinned single crystals of 2H-NbSe₂ (#Z) and CeRu₂. The $\chi'_{3\omega}$ data are recorded in h_{AC} of 3.5 Oe (r.m.s.), whereas the measurements on the noise in χ'_{ω} (see ref. [21] were made with $h_{AC} = 0.5$ Oe (r.m.s.). The $T_p^{\text{on}(ZFC)}$ value in panel (a) corresponds to the said value identified in figure 2b for the same h_{AC} of 3.5 Oe (r.m.s.). The T_{pl} value in panel (b) identifies the onset temperature of the PE in h_{AC} of 0.5 Oe (r.m.s.) in the sample Z, following the nomenclature as in ref. [21]. $T_{pl}(H)$ values denote the boundary of elastic to plastic flow for the driven vortex matter. A comparison of data in panels (b) and (d) shows that T^* values identify limiting temperatures above which $\chi'_{3\omega}$ responses monotonically decrease and the noise signals in χ'_{ω} recede to the respective baselines.

propose that $T_{SMP}^{\text{on}}(H)$ line corresponds to the boundary where pockets of disordered phase start proliferating in the ordered vortex state. However, the fraction of the ordered phase exceeds that of the disordered phase up to T_p^{on} . Above T_p^{on} , the balance starts to rapidly tilt in favor of the disordered regions and the strongly pinned phase starts determining the overall electromagnetic response. Above the spinodal line $T^*(H)$, the phase coexistence and metastability features cease and the sample is homogeneously filled with the disordered regions. The bifurcation of the coexistence phase space into regions I and II, where the order and the disorder dominate, respectively, finds additional support from the temperature dependence of $\chi'_{\omega}(T)$ in the FCW mode in figures 3c and 3d. Both sets of data show that $J_c(T)$ values for the stronger pinned vortex solid continue to decrease between T_{SMP}^{on} and T_p^{on} . It is only above T_p^{on} that the $J_c(T)$ values for ZFC and FCW modes start to increase.

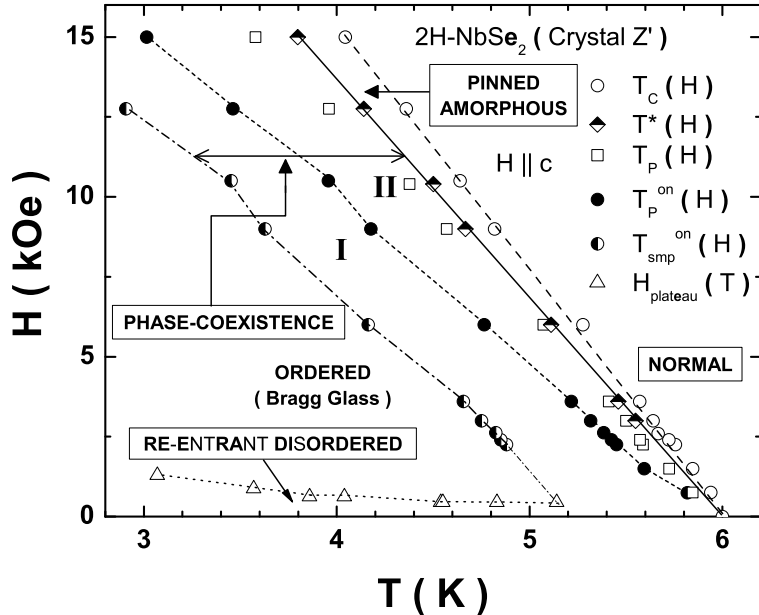


Figure 6. Vortex phase diagram for $H \parallel c$ in a typically weakly pinned single crystal of 2H-NbSe₂. The diagram comprises the values of onset temperatures of the second magnetization peak anomaly ($T_{\text{SMP}}^{\text{on}}$) and the peak effect (T_p^{on}), the value of the peak temperature of the PE (T_p^{ZFC}) in the ZFC mode, the limiting (spinodal) temperature T^* , the $T_c(H)$ and the values of the cross-over field, $H_{\text{plateau}}(T)$, determined from the normalized plots of critical current density vs. normalized fields as in ref. [21]. The (H, T) phase space above $H_{\text{plateau}}(T)$ and below $T_{\text{SMP}}^{\text{on}}(H)$ identifies the ordered Bragg (elastic) glass region. The intervening phase space between $T_{\text{SMP}}^{\text{on}}(H)$ and $T^*(H)$ comprises the coexistence regime of ordered (weaker pinned) and disordered regions. $T_p^{\text{on}}(H)$ values sub-divide the coexistence phase space into regions I and II in which ordered and disordered pockets dominate, respectively. The region I appear continuously connected to the phase space of the so-called reentrant disordered regime, in which vortices are in the small bundle collective pinning regime. The phase space intervening between T^* and T_c identifies the pinned amorphous region.

4. Summary

To summarize, we have investigated the effect of drive and disorder on supercooling/superheating effects across the anomalous variations in critical current density in several single crystals of 2H-NbSe₂ and compared their results with those in a single crystal of CeRu₂. We have mapped out in typically weakly pinned crystals of 2H-NbSe₂ and CeRu₂ the phase coexistence regime of the stronger and the weaker pinned pockets, where metastability effects manifest in a prominent manner. The termination of the phase coexistence regime at higher field and higher temperature

Effect of pinning and driving force on metastability effects

end can be conveniently located in the third harmonic AC susceptibility data. At lower fields ($\lesssim 1$ kOe), the region I of the phase coexistence regime, in which the order dominates, can be seen to continuously connect to the so-called reentrant disordered phase [11,17], where the intervortex spacing presumably exceeds the range of interaction ($a_0 > \lambda$, where λ is the penetration depth). Bitter decoration [41] and simulation studies [42] have shown that the reentrant disordered phase comprises polycrystalline form of flux line lattice. So long as the domains are large, with radial correlation length $R_c \gg a_0$, the weaker pinned regions dominate. The electromagnetic response of the sample and the imposition of the external driving forces can shrink the stronger pinned domain wall regions. However, as the domain sizes shrink on crossing over to the region II of the phase coexistence regime, the external driving forces aid the process of complete amorphization of the vortex matter. The vortices remain pinned in the amorphous region between T^* and T_c values in the typically weakly pinned crystals of low temperature superconductors.

Acknowledgments

We have benefited from discussions with E Y Andrei, S Bhattacharya, C V Tomy, A Tulapurkar, D Pal and D Jaiswal-Nagar. We thank P L Gammel for the crystal Y' of 2H-NbSe₂ and Y Onuki for the CeRu₂ crystal. We also thank R S Sannbhadt and U V Vaidya for technical assistance. One of us (ADT) would like to acknowledge the TIFR Endowment Fund for Kanwal Rekhi Career Development support.

References

- [1] P W Anderson, in *Basic notions of condensed matter physics* (Addison-Wesley Publication Company, USA, 1983)
- [2] M Tinkham, *Introduction to superconductivity*, 2nd ed. (McGraw-Hill International Edition, 1996)
- [3] G Blatter, M V Feigel'man, V B Geshkenbein, A I Larkin and V M Vinokur, *Rev. Mod. Phys.* **66**, 1125 (1994) and references therein
- [4] M Marchevsky, M J Higgins and S Bhattacharya, *Nature (London)* **409**, 591 (2001)
- [5] G Blatter, V B Geshkenbein and J A G Koopmann, *Phys. Rev. Lett.* **92**, 067009 (2004) and references therein
- [6] A B Pippard, *Philos. Mag.* **19**, 217 (1969)
- [7] A I Larkin and Yu N Ovchinnikov, *J. Low Temp. Phys.* **34**, 409 (1979)
- [8] W K Kwok, J A Fendrich, C J van der Beek and G W Crabtree, *Phys. Rev. Lett.* **73**, 2614 (1994)
- [9] M J Higgins and S Bhattacharya, *Physica* **C257**, 232 (1996) and references therein
- [10] A Soibel, E Zeldov, M Rappaport, Y Myasoedov, T Tamegai, S Ooi, M Konczykowski and V B Geshkenbein, *Nature (London)* **406**, 282 (2000)
- [11] S S Banerjee, T V C Rao, A K Grover, M J Higgins, G I Menon, P K Mishra, D Pal, S Ramakrishnan, G Ravikumar, V C Sahni, S Sarkar and C V Tomy, *Physica* **C355**, 39 (2001)
- [12] A I Larkin and Yu V Ovchinnikov, *Sov. Phys. JETP* **38**, 854 (1974)

- [13] T Giamarchi and P Le Doussal, *Phys. Rev.* **B52**, 1242 (1995)
- [14] S S Banerjee, N G Patil, S Ramakrishnan, A K Grover, S Bhattacharya, P K Mishra, G Ravikumar, T V Chandrasekhar Rao, V C Sahni, M J Higgins, C V Tomy, G Balakrishnan and D McK Paul, *Phys. Rev.* **B59**, 6043 (1999)
- [15] S B Roy and P Chaddah, *J. Phys.: Condens. Matter* **9**, L625 (1997); **10**, 4885 (1998)
- [16] G Ravikumar, P K Mishra, V C Sahni, S S Banerjee, A K Grover, S Ramakrishnan, P L Gammel, D J Bishop, E Bucher, M J Higgins and S Bhattacharya, *Phys. Rev.* **B61**, 12490 (2000)
- [17] S S Banerjee, S Ramakrishnan, A K Grover, G Ravikumar, P K Mishra, V C Sahni, C V Tomy, G Balakrishnan, D McK Paul, P L Gammel, D J Bishop, E Bucher, M J Higgins and S Bhattacharya, *Phys. Rev.* **B62**, 11838 (2000)
- [18] A M Troyanovski, M van Hecke, N Saha, J Aarts and P H Kes, *Phys. Rev. Lett.* **89**, 147006 (2002)
- [19] X S Ling, S R Park, B A McClain, S M Choi, D C Dender and J W Lynn, *Phys. Rev. Lett.* **86**, 712 (2001)
- [20] Z L Xiao, O Dogru, E Y Andrei, P Shuk and M Greenblatt, *Phys. Rev. Lett.* **92**, 227004 (2004)
- [21] S S Banerjee, N G Patil, S Saha, S Ramakrishnan, A K Grover, S Bhattacharya, G Ravikumar, P K Mishra, T V Chandrasekhar Rao, V C Sahni, M J Higgins, E Yamamoto, Y Haga, M Hedo, Y Inada and Y Onuki, *Phys. Rev.* **B58**, 995 (1998)
- [22] S Ramakrishnan, S Sundarum, R S Pandit and G Chandra, *J. Phys.* **E18**, 650 (1985)
- [23] S S Banerjee, *Vortex state studies in superconductors*, Ph.D. Thesis (University of Mumbai, Mumbai, 2000)
- [24] S Sarkar, D Pal, S S Banerjee, S Ramakrishnan, A K Grover, C V Tomy, G Ravikumar, P K Mishra, V C Sahni, G Balakrishnan, D McK Paul and S Bhattacharya, *Phys. Rev.* **B61**, 12394 (2000)
- [25] X S Ling and J I Budnick, in *Magnetic susceptibility of superconductors and other spin systems* edited by R A Hein, T L Francavilla and D H Leibenberg (Plenum Press, New York, 1991) p. 377
- [26] Z L Xiao, E Y Andrei, P Shuk and M Greenblatt, *Phys. Rev. Lett.* **86**, 2431 (2001)
- [27] M Steingart, A G Putz and E J Kramer, *J. Appl. Phys.* **44**, 5580 (1973)
- [28] W Henderson, E Y Andrei, M J Higgins and S Bhattacharya, *Phys. Rev. Lett.* **77**, 2077 (1996)
- [29] S Sarkar, D Pal, P L Paulose, S Ramakrishnan, A K Grover, C V Tomy, D Dasgupta, B K Sarma, G Balakrishnan and D McK Paul, *Phys. Rev.* **B64**, 144510 (2001)
- [30] C P Bean, *Phys. Rev. Lett.* **8**, 250 (1962)
- [31] C P Bean, *Rev. Mod. Phys.* **36**, 31 (1964)
- [32] L Ji, H Sohn, G C Spalding, C J Lobb and M Tinkham, *Phys. Rev.* **40**, 10936 (1989)
- [33] Y Yeshurun, M W McElfresh, A P Malozemoff, J Hagerhorst-Trehella, J Mannhart, F Holtzberg and G V Chandrashekhar, *Phys. Rev.* **B42**, 6322 (1990)
- [34] P Chaddah, S B Roy, Shailendra Kumar and K V Bhagwat, *Phys. Rev.* **B46**, 11737 (1992)
- [35] Shailendra Kumar, S B Roy, P Chaddah, Ram Prasad and N C Soni, *Physica* **C191**, 450 (1992)
- [36] G Ravikumar, V C Sahni, A K Grover, S Ramakrishnan, P L Gammel, D J Bishop, E Bucher, M J Higgins and S Bhattacharya, *Phys. Rev.* **B63**, 024505 (2001)
- [37] A C Marley, M J Higgins and S Bhattacharya, *Phys. Rev. Lett.* **74**, 3029 (1995)
- [38] R Merithew, M W Rabin, M B Weissman, M J Higgins and S Bhattacharya, *Phys. Rev. Lett.* **77**, 3197 (1996)

Effect of pinning and driving force on metastability effects

- [39] D Li and B Rosenstein, *Phys. Rev.* **B65**, 220504 (2002), cond-mat/0305258
E Y Andrei, Z L Xiao, W Henderson, Y Paltiel, E Zeldov, M J Higgins,
S Bhattacharya, P Shuk and M Greenblatt, *Condensed matter theories* (Nova Science Publishers, New York, USA, 2001) vol. 16, pp. 241–252
- [40] A D Thakur, S S Banerjee, M J Higgins, S Ramakrishnan and A K Grover, *Phys. Rev.* **B72**, 134524 (2005)
- [41] M Menghini, Y Fasano and F de la Cruz, *Phys. Rev.* **B65**, 064510 (2002)
- [42] M Chandran, R T Scalettar and G T Zimnyi, *Phys. Rev.* **B69**, 024526 (2004)